Cell Death and Differentiation (2008) 15, 1794–1803

www.nature.com/cdd

Intersubunit interactions between mutant DEG/ENaCs induce synthetic neurotoxicity

W Zhang[1,3], L Bianchi[2,3], W-H Lee[1], Y Wang[2], S Israel[1] and M Driscoll*[1]

Ion channel hyperactivation can result in neuronal loss in injury, stroke and neurodegenerative disease. Acidosis-associated hyperactivation of the Degenerin/epithelial amiloride-sensitive Na^+ channel (DEG/ENaC) acid-sensing ion channel 1a (ASIC1a), a proton-gated channel expressed in the mammalian brain, contributes significantly to neuronal loss in ischemia. Analogously, in invertebrates, genetic hyperactivation of the *Caenorhabditis elegans* mechanosensory (MEC) channel (MEC-4(d)) of the DEG/ENaC ion channel superfamily induces neuronal necrosis. Similarly substituted MEC-10(d) mutant subunits of the same MEC channel are only marginally neurotoxic, and we therefore exploited the weak necrosis phenotype of *mec-10(d)* lines to screen for novel extragenic mutations that enhance neuronal death. Here, we report on one *mec-10(d)* necrosis enhancer, which we show is MEC-4 variant MEC-4(A149V). MEC-4(A149V) executes normal MEC-4 function in touch sensation and does not induce necrosis on its own, but rather combines with MEC-10(d) to create a strongly neurotoxic channel. The MEC-4(A149V) + MEC-10(d) channel conducts elevated Na^+ and Ca^{2+} currents (with a disproportionate increase in Ca^{2+} current) in the *Xenopus* oocyte expression system, and exhibits altered binding of the channel inhibitor amiloride. Our data document the first example of synergistically toxic intersubunit interactions in the DEG/ENaC channel class and provide evidence that Ca^{2+} current levels may be decisive factors in tipping the balance between neuronal survival and necrosis.
Cell Death and Differentiation (2008) **15,** 1794–1803; doi:10.1038/cdd.2008.114; published online 1 August 2008

Ion channel dysfunction can result in the neuronal death that underlies the devastating consequences of stroke and nervous system injury. Primary determinants of mammalian neuronal loss associated with ion channel hyperactivation include the glutamate-gated channels[1] and the less extensively studied ASIC (acid-sensing ion channels)[2] of the DEG/ENaC superfamily (named after founding members *Caenorhabditis elegans* degenerins and the mammalian epithelial amiloride-sensitive Na^+ channels). DEG/ENaC channel complexes include three DEG/ENaC subunits,[3] with each subunit having a large extracellular domain, two transmembrane domains that contribute to the channel pore, and intracellular N and C termini (reviewed in Kellenberger and Schild[4]). Structure/activity studies in the DEG/ENaC channel class have provided insights into function, but the relationship between toxicity and subunit interactions is largely unexplored.

Of DEG/ENaCs studied to date, the *C. elegans* MEC channel, which transduces gentle touch stimuli in six mechanosensory (MEC) neurons[5,6] has been analyzed in most genetic detail. The core of the MEC channel is formed by DEG/ENaC subunits MEC-4[7,8] and MEC-10,[9] which associate with paraoxonase-like transmembrane protein MEC-6[10] and stomatin-like protein MEC-2.[7,11,12] Dominant gain-of-function mutations alter MEC-4(A713) (the *d* position) to introduce large amino acids (AAs) near the channel pore, causing channel hyperactivity that induces necrotic-like neurodegeneration.[8,11,13] Analogous substitutions for MEC-10 (MEC-10(d), position A673) are only weakly neurotoxic.[9] Neurotoxic MEC-4(d) channels conduct both elevated Na^+ and Ca^{2+} currents[13] and exhibit commonalities with the hyperactivation of the Na^+- and Ca^{2+}-permeable mammalian ASIC1a channel,[14] which, when overstimulated by brain acidosis in ischemia, causes neurodegeneration.[2] Understanding mechanisms by which neuronally expressed DEG/ENaCs are hyperactivated to become toxic is thus of considerable significance in pathobiology.

To elaborate molecular mechanisms of channel neurotoxicity within a physiological context, we screened for new extragenic mutations that enhance the weak *mec-10(d)*-induced neurodegeneration. Here, we report on death enhancer allele *bz301*, which we show is a novel *mec-4* allele encoding MEC-4(A149V) substitution in the channel extracellular domain. MEC-4(A149V) functions normally in touch sensation and induces neurodegeneration only in combination with the MEC-10(d) subunit. Our electrophysiological analysis supports that the MEC-4(A149V) + MEC-10(d) channel is hyperactivated and preferentially calcium perme-

[1]Department of Molecular Biology and Biochemistry, Rutgers University, Piscataway, NJ, USA and [2]Department of Physiology and Biophysics, University of Miami School of Medicine, Miami, FL, USA
*Corresponding author: M Driscoll, Department of Molecular Biology and Biochemistry, Rutgers University, Nelson Biological Laboratories, Room A232, Piscataway, NJ 08854, USA. Tel: 732 445 7182; Fax: 732 445 7192; E-mail: driscoll@biology.rutgers.edu
[3]These two authors contributed equally to this work.
Keywords: necrotic cell death; neurodegeneration; *Caenorhabditis elegans*; channel structure
Abbreviations: AA, amino acid; ASICs, acid-sensing ion channels; COPAS BIOSORT, Complex Object Parametric Analyzer and Sorter; CRD, Cys-rich domain; DEG/ENaCs, Degenerin/epithelial amiloride-sensitive Na^+ channels; EMS, ethyl methyl sulfonate; GFP, green fluorescent protein; L1–L4, larval stages 1–4; MEC, mechanosensory; MSD, membrane-spanning domain; N2, wild-type *C. elegans* strain-Bristol isolate; PLM, posterior lateral microtubule neurons; SNIP, single nucleotide polymorphism; WT, wild type
Received 07.2.08; revised 19.5.08; accepted 28.5.08; Edited by P Nicotera; published online 01.8.08

able, with altered amiloride binding properties. These data inform on quaternary channel relationships and provide an example of intersubunit interaction toxicity that suggests that allelic variation within the mammalian ASIC channel class might influence susceptibility to ischemia.

Results

A screen for enhancers of *mec-10(d)*-induced neurodegeneration. We constructed a strain that expresses both transgenically introduced *mec-10(d)*[9] and a green fluorescent protein (GFP) reporter (to highlight touch neurons) in the touch neurons (we named this strain *lsmec-10(d)*). We evaluated survival of touch neurons in *lsmec-10(d)* at the larval stage 4 (L4)/young adult stage by scoring the numbers of fluorescent posterior lateral microtubule neurons (PLM) in the tail, which are positioned away from the gut autofluorescence and are, thus, unambiguously identified (Figure 1a). In nematodes reared at 20°C, most PLM neurons in *lsmec-10(d)* are viable despite the expression of weak necrosis inducer *mec-10(d)*. *lsmec-10(d)* does exhibit some necrosis at 15°C, confirming the potential for necrosis induction by the *mec-10(d)* transgene array (Figure 1a). We mutagenized parental line *lsmec-10(d)* by ethyl methyl sulfonate (EMS) treatment, and screened

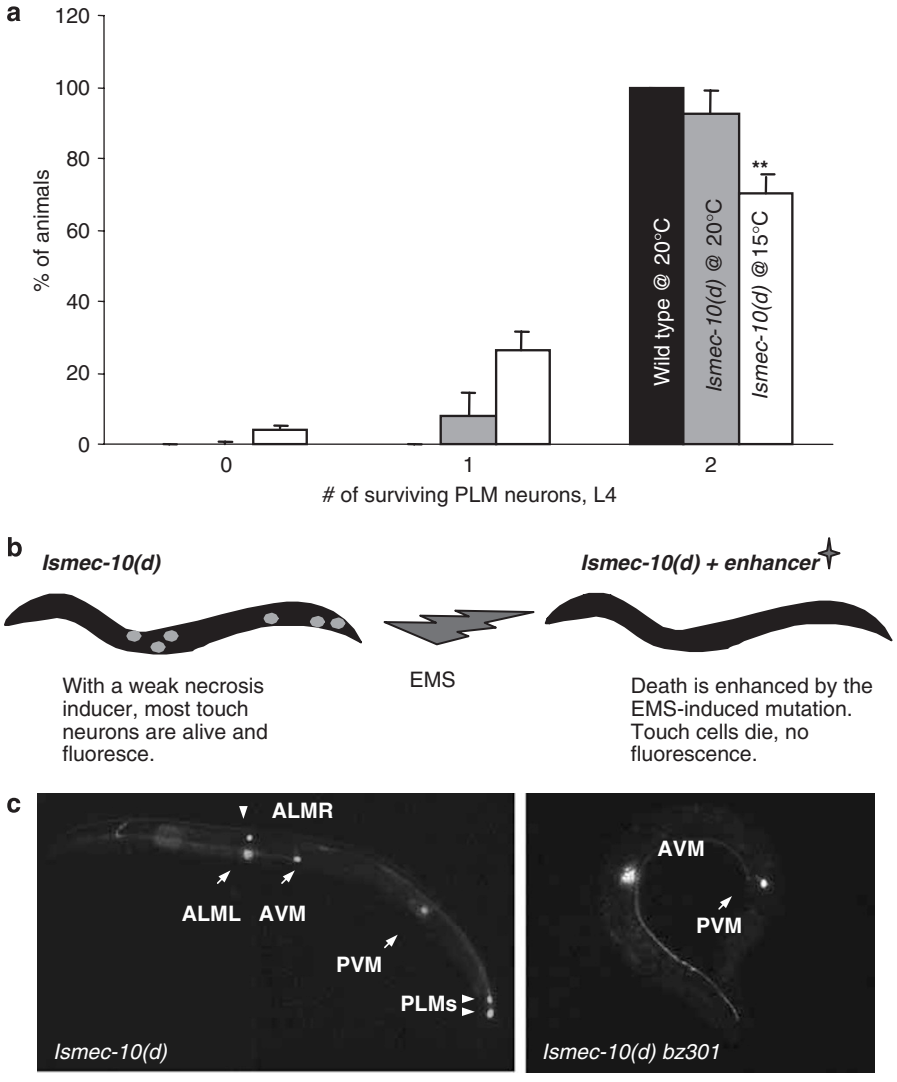

Figure 1 A green fluorescent protein (GFP)-based screen for the enhancers of neurodegeneration induced by transgene *mec-10(d)*. (**a**) Quantitation of touch cell loss in parental strain *lsmec-10(d)*. *mec-10(d)* induces marginal necrosis in touch neurons at 20°C, but is more toxic at 15°C. The *X* axis indicates how many of the two PLM neurons (0, 1, or 2) can be detected in wild type (WT; black bar) and in *lsmec-10(d)* at 20°C (gray) or at 15°C (white). $n = 700$ (in seven independent trials) at 20°C and $n = 400$ (in four independent trials) at 15°C; $^{**}P < 0.01$ by comparison with WT, by *t*-test. These data establish that *lsmec-10(d)* has the potential to induce necrosis, but exhibits a low baseline of cell death at 20°C. (**b**) Strategy for identifying enhancers of *mec-10(d)*-induced neurodegeneration. In the parental strain *lsmec-10(d)* (which is *zdIs5[$p_{mec\text{-}4}$GFP] I; bzIs67[mec-10(d)] X)*, there is actually little necrosis, and thus the six touch receptor neurons almost always survive and fluoresce. Mutants that harbor a new necrosis enhancer mutation consequent to ethyl methyl sulfonate (EMS) treatment will have less GFP signal due to touch receptor neuron death. (**c**) An example of touch receptor fluorescence in the parental strain (left panel) and in the *bz301* enhancer mutant background (right panel). In the *bz301* strain, four touch neurons have died and only AVM and PVM survive

18 500 genomes for novel mutants lacking some or all of the fluorescent touch neurons, revealing enhanced neuronal loss (Figure 1b and c). We identified 18 mutants that exhibit strong/intermediate enhancement of necrosis, as well as several weaker death enhancers. Here, we describe molecular identification and characterization of *bz301*, one of the strong necrosis enhancers (Figure 1c, right panel).

***bz301* is a semi-dominant enhancer of *lsmec-10(d)* that exacerbates necrosis in a calreticulin-dependent mechanism.** In the *lsmec-10(d) bz301* mutant (20°C), 49% of young L1 larvae have one to two necrotic PLMs (Figure 2a), and yet 84% lack one to two PLMs by the L4 stage (Figure 2b). The fact that more neurons are dead by the L4 stage than appear dying at the L1 stage suggests that necrosis onset can be after the L1 stage in the *lsmec-10(d) bz301* strain, and we confirmed this by visual inspection of L2 and L3 larvae that were devoid of swollen necrotic neurons as L1s (data not shown). Although *bz301* is a strong necrosis enhancer, its effects are less potent than observed for *mec-4(d)* – in *mec-4(d)* mutants, 95% of L1 larvae have one to two necrotic PLM neurons and 100% have either 1 or 2 neurons dead by the L4 stage. We find a significant amount of death in the *bz301/+* heterozygotes, which approaches that in *bz301/bz301* homozygotes (Figure 2c). These results establish the genetically semi-dominant action of allele *bz301* in necrosis enhancement.

We also tested whether enhancer *bz301* activates necrosis with similar genetic requirements to *mec-4(d).* In *mec-4(d)*-induced death, progression through necrosis requires calreticulin, a calcium-storing ER (endoplasmic reticulum) chaperone, which we propose is needed for the release of ER calcium stores and amplification of toxic Ca^{2+} overload.[15] We constructed the triple mutant *crt-1; lsmec-10(d) bz301* to ask whether the enhanced death is blocked by the *crt-1* null mutation. We found that calreticulin deficiency fully blocks necrosis-enhancing effects of *bz301* (Figure 2a and b). We concluded that *bz301*-induced necrosis involves a mechanism similar to that induced by the MEC-4(d) channel.

Necrosis enhancer *bz301* encodes MEC-4(A149V), adjacent to a conserved extracellular domain. One class of necrosis enhancer that could have been identified in our screen could include *mec-4* mutations that themselves induce necrosis.[8,16] As our genetic mapping placed *bz301* on the X chromosome near *mec-4*, we sequenced the *mec-4* coding sequence in this mutant background. We found that *bz301* does encode a *mec-4* mutation, distinct from previously sequenced *mec-4* alleles,[17,18] specifying AA change A149V (Figure 3). A149 is located 19 AAs from MEC-4 membrane-spanning domain I (MSDI) on the extracellular side of the protein, adjacent to a conserved DEG/ENaC domain of unknown function (Figure 3a and b). This residue is commonly a nonpolar residue or an Ala (in 32 out of 40 family members; Figure 3b and Supplementary Figure 1), and 4 DEG/ENaC family members (snail FaNaC, *C. elegans* DEG-1, and two uncharacterized *C. elegans* family members) normally encode Val at this position (Supplementary Figure 1). Interestingly, this region was found to be a site of interaction between two adjacent

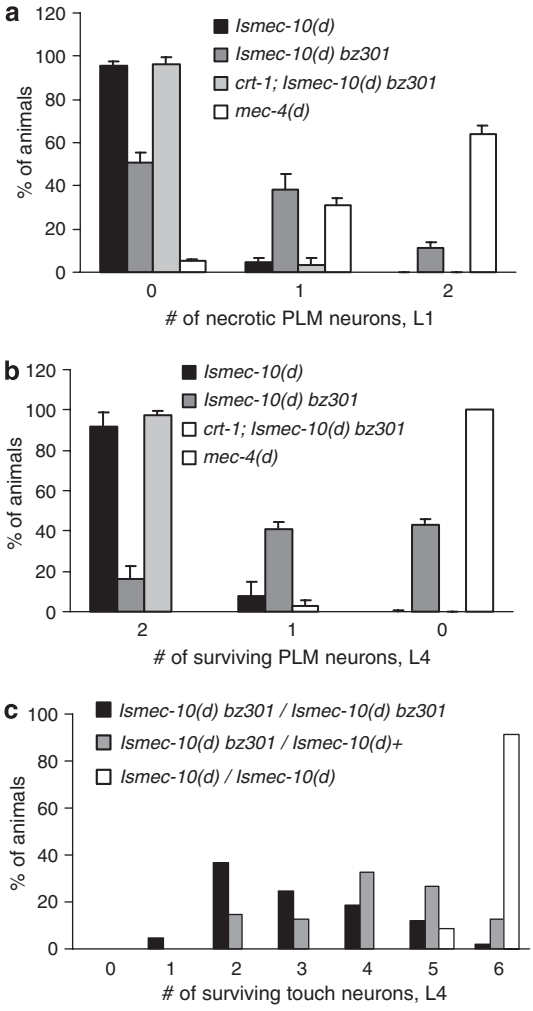

Figure 2 *bz301* acts semi-dominantly to enhance neuronal loss in *lsmec-10(d)* by a calreticulin-dependent mechanism. (**a**) Quantitation of swollen necrotic PLM touch neurons during the early L1 stage (within 4 h after hatching) in *lsmec-10(d)* (black), *lsmec-10(d) bz301* (dark gray), *crt-1(bz29); lsmec-10(d) bz301* (light gray), and *mec-4(d)* (white) animals; $n \geqslant 230$ in at least three independent trails, at 20 °C. (**b**) Quantitation of surviving fluorescent PLM touch neurons at the L4 stage for *lsmec-10(d)* (black), *lsmec-10(d) bz301* (dark gray), *crt-1(bz29); lsmec-10(d) bz301* (light gray), and *mec-4(d)* (white) animals. A comparison of the extent of PLM swelling and PLM death for *lsmec-10(d) bz301* reveals that more PLMs die than appear as swollen necrotic figures in the L1 stage, suggesting that neurodegeneration can have late larval onset, and we confirmed this by visual inspection of older larvae (data not shown); $n \geqslant 170$ in at least three independent trails, at 20°C. The *crt-1* null mutation suppresses cell death induced in *lsmec-10(d) bz301.* (**c**) *bz301* acts semi-dominantly. We counted the number of surviving touch receptor neurons (of six total) in *bz301* homozygotes (black) or *bz301* heterozygotes (gray). *lsmec-10(d)* is homozygous in all lines. *bz301* heterozygotes and homozygotes have extensive neuronal loss, but nearly all *lsmec-10(d)* homozygotes (white) have six touch cells surviving

subunits within the trimeric channel complex in the recently solved ASIC1a structure.[3]

To confirm that the *bz301*-encoded *mec-4* mutation is causative for necrosis enhancement, we constructed an *mec-4(bz301)* allele by site-directed mutagenesis and introduced the p*mec-4(bz301)* allele into the *lsmec-10(d)* background (Figure 3c). We find that p*mec-4(bz301)* induces necrosis. We

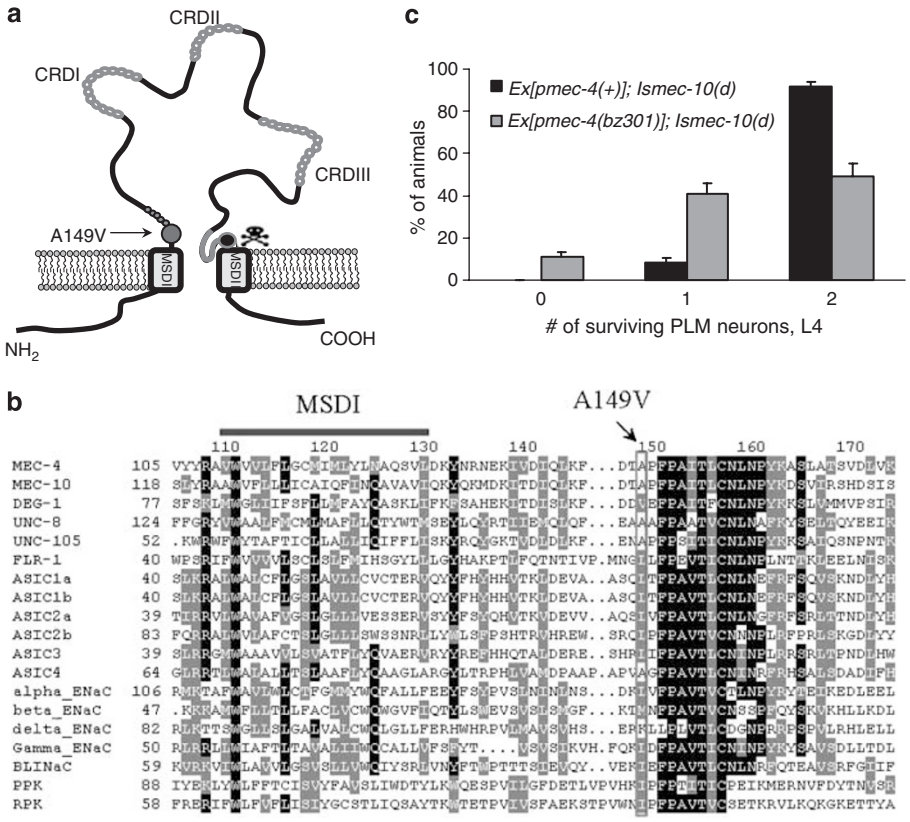

Figure 3 *bz301* is a *mec-4* allele that encodes A149V substitution adjacent to a highly conserved extracellular domain. (**a**) Cartoon representing the transmembrane topology of the MEC-4 subunit and the position of the A149V substitution. Relatively, short N- and C-terminal MEC-4 domains project into the cell and a single large central loop containing three conserved cysteine-rich domains (CRDI, II, and III) extends extracellularly. The A149 position is indicated by a light gray dot and an arrow. The highly conserved region right after A149 is indicated in dark gray. A short loop preceding membrane-spanning domain II (MSDII) is believed to participate in pore formation (gray) and MSDII contributes to the channel pore. The highly conserved *d* position MEC-4(A713) at which large side chain amino acid (AA) substitution hyperactivates the channel is indicated by a black dot. Not all domains are drawn to scale. (**b**) AA sequence alignment of MEC-4 and several DEG/ENaC family members in the region corresponding to MEC-4(A149). The AA change specified by *mec-4* allele *bz301* is noted at the position indicated by an arrow and a box, AA numbers correspond to MEC-4 primary sequence, position of membrane-spanning domain I is indicated. Included in the alignment are some better-studied *C. elegans* family members, human ASICs and ENaCs, and fly PPK-1 and RPK-1. Residues common to all DEG/ENaCs are boxed in black; similar residues are boxed in gray. (**c**) Confirmation that *bz301* is the causative mutation for neurodegeneration. The necrosis-enhancer property is also observed for an engineered transgene *bzEx170[pmec-4(bz301)]* (gray) introduced into the *lsmec-10(d)* background but not *bzEx177[pmec-4(+)]* (black), supporting that the necrosis-enhancer property is conferred by the *bz301* mutation

conclude that the MEC-4(A149V) change is responsible for necrosis-enhancer activity.

***mec-4(bz301)* requires *lsmec-10(d)*, but not *mec-10(+)*, to induce necrosis.** *mec-4(bz301)* might potentiate neurotoxicity of *lsmec-10(d)* or, alternatively, *mec-4(bz301)* could encode a novel mutation that causes necrosis on its own. To distinguish between these two possibilities, we crossed *mec-4(bz301)* away from *lsmec-10(d)* and we scored for touch neuron viability in the *mec-4(bz301)*-only background. We found that *mec-4(bz301)* does not confer neurotoxicity when present in an otherwise wild-type (WT) background (Figure 4a). Importantly, when we reintroduced a *mec-10(d)* integrated transgene array different from the one used to generate the parental *lsmec-10(d)* strain into the *bz(301)* strain, we found that the neurodegeneration phenotype was restored (Figure 4a). These experiments demonstrate that *mec-4(bz301)* must act together with *mec-10(d)* to enhance necrosis and that the neurodegeneration phenotype does not depend on any unusual features of the *mec-10(d)* transgene array that might have been introduced into the original enhancer mutant background by mutagenesis.

In the combinatorial toxicity situation we characterize for *mec-4(bz301)+mec-10(d)*, the strains we initially tested for neurodegeneration also have two WT genomic copies of *mec-10*. To address whether *mec-10(+)* activity is required for synthetic neurotoxicity, we replaced the genomic *mec-10(+)* copies with *mec-10* null deletion allele *tm1552*, while leaving the *mec-10(d)* gene array in place. We found that eliminating *mec-10(+)* alters neither *lsmec-10(d)*- nor *lsmec-10(d); mec-4(bz301)*-mediated neuronal degeneration (Supplementary Figure 2A). We conclude that synthetic neurotoxicity requires only mutant MEC-4(A149V) and MEC-10(d) subunits, presumably as components of a hyperactivated heteromeric DEG/ENaC channel.

MEC-4(A149V) functions normally in touch sensation. *mec-4(+)* is required for sensitivity to gentle touch[8] and contributes to the pore of the mechanotransducing

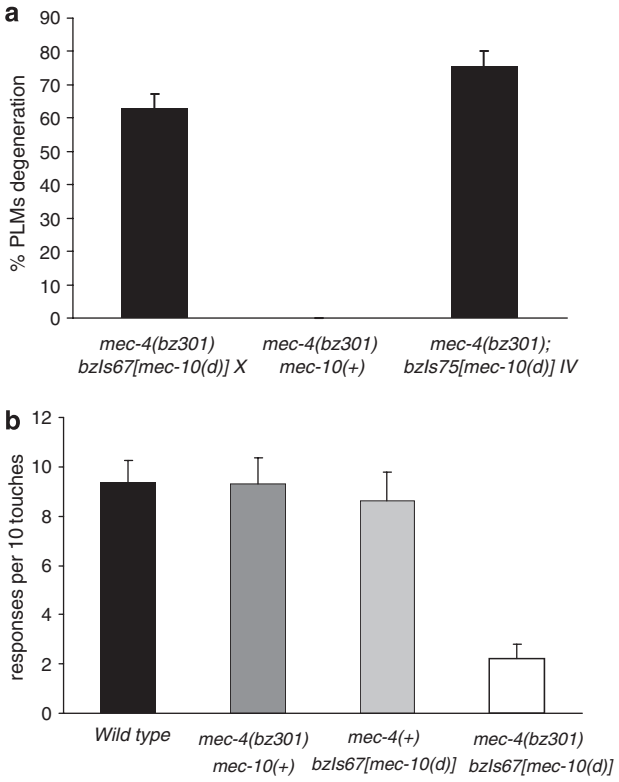

Figure 4 *mec-4(bz301)* encodes a functional MEC-4 subunit that requires *lsmec-10(d)* for neurotoxicity. (**a**) *mec-4(bz301)* is neurotoxic only in conjunction with *lsmec-10(d)*. *bzIs67 X* and *bzIs75 IV* are two independently isolated integrated arrays of *mec-10(d)*, and both are neurotoxic when combined with *mec-4(bz301)*. *Y* axis indicates the percentage of PLM neurons that undergo degeneration by the L4 stage; $n \geqslant 170$ in at least three independent trials, at 20°C. All lines have the GFP transgene labeling the six touch neurons (data not shown). MEC-4(A149V) needs MEC-10(d) for its necrotic effect, but cannot induce cell death on its own. (**b**) The MEC-4(A149V) subunit is a functional MEC-4 subunit. We assayed touch sensitivity of WT (black), *mec-4(bz301)* (dark gray), b*zIs67[mec-10(d)]* (light gray), and *mec-4(bz301) bzIs67[mec-10(d)]* (white) at the L4 stage. We touched animals 10 times and recorded the number of avoidance responses for each animal, $n = 30$, three independent trials performed, at 20°C. As *mec-4(bz301)* exhibits normal touch sensitivity, the MEC-4(A149V) subunit is functional *in vivo*. Note that the combinatorial touch insensitivity of *mec-4(bz301)* and *mec-10(d)* is consistent with their combinatorial degeneration action

complex.[19] We wondered whether the MEC-4(A149V) mutant subunit, which does not kill touch neurons on its own, might still possess functional MEC-4 activity. We compared touch sensitivity of WT and *mec-4(bz301)* mutants to show that touch responses are, in fact, normal in the *mec-4(bz301)* mutant (Figure 4b, dark gray bar). In the *lsmec-10(d);mec-4(bz301)* double mutant, the touch response is impaired (Figure 4b, white bar), most likely the consequence of touch receptor degeneration (*lsmec-10(d)* does not disrupt function on its own (Supplementary Figure 2B). Thus, MEC-4(A149V) is not only non-neurotoxic on its own but also serves as a functional MEC-4 channel subunit.

Overall, we conclude that *mec-4(bz301)* encodes MEC-4 AA change A149V, which is neither neurotoxic nor channel-disrupting on its own *in vivo*, but can combine with the *lsmec-10(d)*-encoded MEC-10(A673V) mutant subunit to generate a strongly neurotoxic channel.

MEC-4(A149V) increases Na^+ currents of MEC homomeric and heteromeric channel complexes. The *C. elegans* MEC channel MEC-4(d) + MEC-10(d) + MEC-2 + MEC-6 has been electrophysiologically characterized in *Xenopus* oocytes[10,11,13,20] (see also Figure 5a). In brief, this work showed that (1) channels including the MEC-4(d) subunit conduct markedly elevated Na^+ and Ca^{2+} currents relative to MEC-4(+) channels (note that MEC-4(+) conducts only barely detectable currents); (2) MEC-10(+) and MEC-10(d) do not conduct current as homomeric channels; (3) MEC-10 is not essential for MEC-4(d) channel conductance and dampens MEC channel currents when present; and (4) stomatin MEC-2 and paraoxonase-related MEC-6 subunits increase current.

To gain insight onto the mechanism by which MEC-4 (A149V) impacts channel function and promotes neurodegeneration in conjunction with MEC-10(d), we asked how this mutant subunit alters MEC channel properties in the oocyte expression system. We tested combinations of MEC-4 and MEC-10 variant subunits in experiments that included MEC-2 and MEC-6 (Figure 5a and b). Consistent with previous findings, neither MEC-4(+) homomeric channels nor MEC-10(d) homomeric channels conduct significant Na^+ current. Similarly, the heteromeric MEC-4(+) + MEC-10(d) channel conducts only marginal Na^+ current. By contrast, the MEC-4(d) + MEC-10(d) channel is dramatically hyperactivated, conducting about 26 μA of Na^+ current.

How do channels harboring the MEC-4(A149V) subunit compare? In control experiments, we confirmed that MEC-2 and MEC-6 influence the MEC-4(A149V) channel similarly to their influence on the MEC-4(d) channel (Supplementary Figure 3A), indicating that basic subunit interactions within the MEC complex appear maintained. We do note three distinctive differences associated with the expression of MEC-4(A149V) subunits. The first difference is that the homomeric MEC-4(A149V) channel is modestly hyperactivated, conducting currents that are still small (1.2 μA), but are, nonetheless, $\sim$10 times larger than those of the MEC-4(+) homomeric channel (Figure 5b and Goodman *et al*.[11]). This finding suggests that the MEC-4(A149V) substitution might alter homomeric channel open probability or pore conductance properties. We note that if a similar increase in overall channel conductance is associated with a native homomeric MEC-4(A149V) channel *in vivo* (in the *mec-10(+)* background), the levels of elevated ion conductance must not reach the threshold for neurotoxicity, because the *mec-10(+);mec-4(bz301)* double mutant does not exhibit neurodegeneration (Supplementary Figure 2A).

Consistent with the previously reported current-suppressing effect of MEC-10(+) on MEC-4(d) currents,[11,13,20] we find that the coexpression of MEC-4(A149V) with MEC-10(+) is associated with currents that are smaller relative to MEC-4(A149V) alone. If the native MEC-4(A149V) + MEC-10(+) channel has altered electrophysiological properties *in vivo*, changes are not substantial enough to disrupt the function in touch sensation, as the *mec-4(bz301)* mutant is touch sensitive and *mec-4* function is required for this behavior (Figure 4b).

The second major difference associated with the MEC-4(A149V) channel involves the heteromeric MEC-

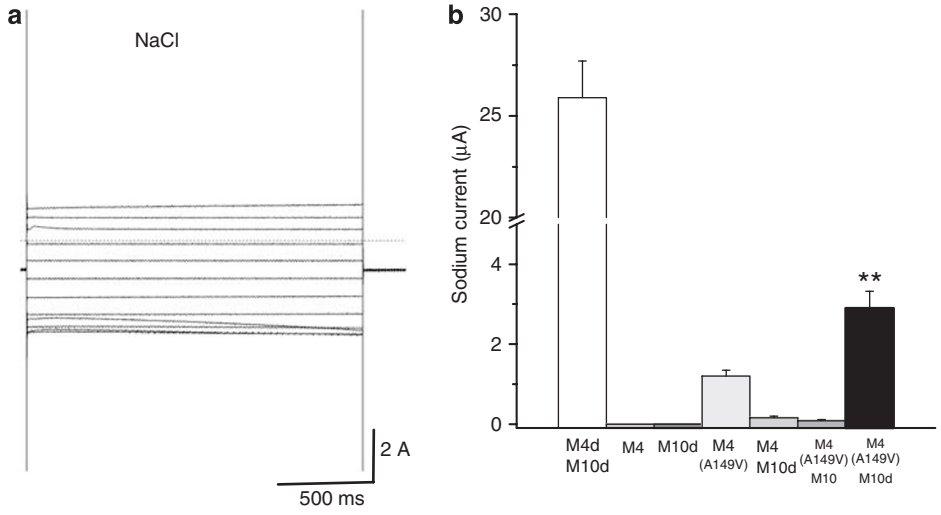

Figure 5 MEC-4(A149V) death-enhancer channel subunits increase currents through MEC-10(d) channels in *Xenopus* oocytes. (**a**) An example of sodium currents elicited by voltage steps from −160 to + 60 mV from a holding potential of −30 mV in an oocyte injected with *mec-4(A149V)*, *mec-10(d)*, and *mec-2* and *mec-6* and exposed to a NaCl solution. (**b**) The average Na^+ current at −160 mV recorded from oocytes injected with the subunit compositions indicated on the *X* axis. In all injections, MEC-2 and MEC-6 cRNA were added to the MEC-4 and/or MEC-10 channel subunit cRNAs. *n* was 5–21. Data are expressed as mean ± SE. $^{**}P < 0.01$ by comparison with all the other channel compositions, by *t*-test

4(A149V) + MEC-10(d) combination, which we have shown is toxic *in vivo*. We find that the current of the MEC-4(A149V) + MEC-10(d) channel is markedly elevated relative to the MEC-4(+) + MEC-10(d) channel, exhibiting ~15 times higher Na^+ currents. This current elevation demonstrates a synergistic activation in the heteromeric MEC-4(A149V) + MEC-10(d) channel that could explain the observed combinatorial toxicity *in vivo*. The third major difference is the change in amiloride binding of the MEC-4(A149V) + MEC-10(d) heteromeric channel (Supplementary Figure 4), suggesting that both MEC-4 and MEC-10 DEG/ENaC subunits participate in forming the high-affinity amiloride binding site in the channel pore.[11,13]

We conclude the MEC-4(A149V) + MEC-10(d) channel is hyperactivated, although to a lesser extent than the MEC-4(d) + MEC-10(d) channel. Interestingly, the conductance levels of the heterologously expressed MEC-4 + MEC-10(d) channels parallel the severity of toxicity seen *in vivo* – the MEC-4(A149V) + MEC-10(d) channel exhibits later onset neurodegeneration and is less toxic than the MEC-4(d) + MEC-10(d) channel *in vivo* (Figure 2a and b). Like the MEC-4(d) channel, the MEC-4(A149V) channel induces death of *Xenopus* oocytes (Supplementary Figure 3B).

In summary, the MEC-4(A149V) substitution alone can change MEC channel complex Na^+ conductance properties modestly, but in conjunction with MEC-10(d), Na^+ currents are significantly increased.

MEC-4(A149V) increases Ca^{2+} currents of MEC homo- and hetero-multimeric channel complexes. In our previous studies, we found that elevated Ca^{2+} permeability correlated with MEC-4(d) channel neurotoxicity,[13] and therefore we evaluated the Ca^{2+} conduction of MEC-4(A149V)-containing channels. When *Xenopus* oocytes expressing the MEC-4(d) channel complex are bathed in a $CaCl_2$ solution, the Ca^{2+} current conducted by the MEC channel activates an oocyte-endogenous Ca^{2+}-activated Cl^- channel.[13] The activation of the endogenous Ca^{2+}-activated Cl^- channel thus serves as an indirect measure of MEC channel Ca^{2+} permeability.

When we perfused oocytes expressing homomeric MEC-4(+) or homomeric MEC-4(A149V) channels with a $CaCl_2$ solution, we did not observe the induction of the Ca^{2+}-activated Cl^- current, indicating that neither MEC-4(+) nor MEC-4(A149V) channels are permeable to significant Ca^{2+} currents in the absence of MEC-10(d) (Figure 6b). By contrast, we find that the MEC-4(A149V) + MEC-10(d) channel activates the *Xenopus* oocyte endogenous Ca^{2+}-activated Cl^- current significantly (Figure 6a and b),[13] establishing that channels formed by MEC-4(A149V) + MEC-10(d) are Ca^{2+} permeable and, in this assay, showing that the neurotoxic channel conducts more Ca^{2+} than the WT channel. The level of current induction in the MEC-4(A149V) + MEC-10(d) channel is less than that induced by the MEC-4(d) + MEC-10(d) (measuring ~20% of the MEC-4(d) + MEC-10(d) channel), paralleling *in vivo* data on relative toxicity of MEC-4(A149V) + MEC-10(d) *versus* MEC-4(d).

To examine Ca^{2+} currents of MEC-4(A149V)-containing channels more quantitatively, we perfused oocytes containing MEC-10(d) + either MEC-4(A149V) or MEC-4(d) with a $CaCl_2$ solution and simultaneously blocked the endogenous Ca^{2+}-activated Cl^- current by injecting EGTA into the oocytes. Previously, we showed that the MEC-4(d) channels, but not the MEC-4(+) channels, induce a detectable Ca^{2+} current in this assay.[13] When we measure the MEC channel Ca^{2+} current directly, we find that MEC-4(A149V) + MEC-10(d) Ca^{2+} currents are indeed detectable and are ~25% of those of the MEC-4(d) + MEC-10(d) channel (Figure 6d). We conclude that the combinatorial MEC-4(A149V) + MEC-10(d) channel conducts elevated Ca^{2+}, whereas channels including either MEC-4(+) or MEC-10(+) do not.

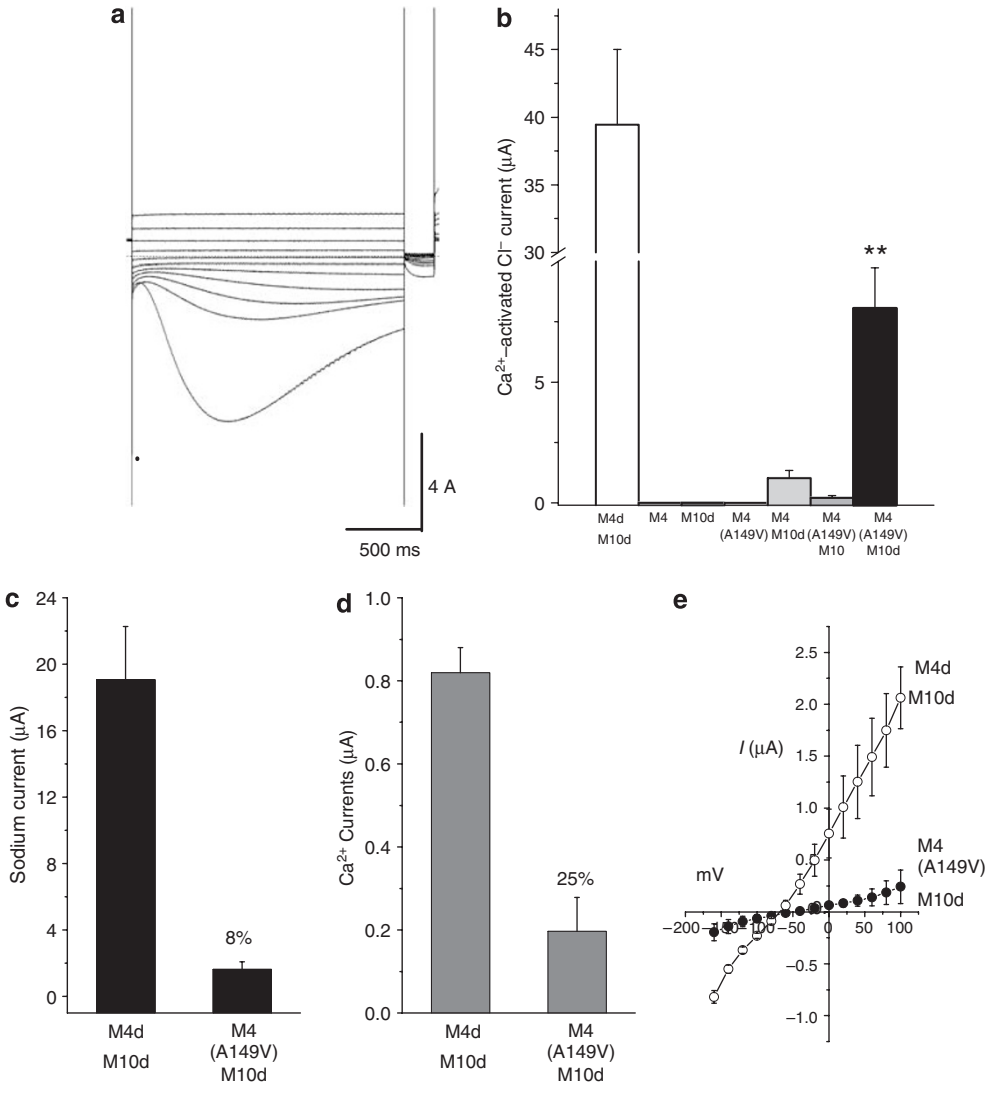

Figure 6 MEC-4(A149V) + MEC-10(d) channels exhibit enhanced Ca^{2+} currents without a change in Ca^{2+} permeability. (**a**) The same oocyte shown in Figure 5a was exposed to the Ca^{2+} solution, resulting in the activation of the endogenous Ca^{2+}-activated Cl^- current. (**b**) Average Ca^{2+}-activated Cl^- current at -160 mV for the subunit combinations indicated (+ MEC-2 and MEC-6). Note that for MEC-4(A149V) + MEC-10(d), both Na^+ currents and Ca^{2+}-activated Cl^- currents, which are a measure of the amount of Ca^{2+} permeating through the channel, are bigger than all the other channel combinations except MEC-4(d) + MEC-10(d). Data are expressed as mean ± SE. $^{**}P<0.01$ by comparison with all the other channel compositions, by *t*-test. (**c**) Average Na^+ current at −160 mV from oocytes injected with MEC-4(d) + MEC-10(d) and MEC-4(A149V) + MEC-10(d) (+ MEC-2 and MEC-6). Note that in this batch of oocytes, Na^+ currents produced by the expression of MEC-4(A149V) + MEC-10(d) are only 8% of currents produced by the expression of MEC-4(d) + MEC-10(d). (**d**) The average Ca^{2+} currents at −160 mV for the same subunit combinations shown in panel a. MEC-4(A149V) + MEC-10(d) channels produce Ca^{2+} currents that are 25% of currents produced by the expression of MEC-4(d) + MEC-10(d). We compared Na^+ and Ca^{2+} current ratios by Student's *t*-test and we also found that the ratios to be statistically different ($P \leqslant 0.05$). The difference in the size of the Na^+ and Ca^{2+} currents as compared with MEC-4(d) + MEC-10(d) might suggest that MEC-4(A149V) affects permeability, conductance, or open probability of the channel complex when conducting Ca^{2+} and Na^+ currents in two distinct ways. (**e**) Current–voltage relationship of Ca^{2+} currents is measured using the EGTA injection protocol in oocytes expressing MEC-4(d) + MEC-10(d) (open circles) and MEC-4(A149V) + MEC-10(d) (+ MEC-2 and MEC-6). The reversal potentials of the Ca^{2+} currents were not statistically different (−65 ± 5.07, $n=5$ *versus* −70 ± 7.83, $n=13$, respectively). This result indicates that Ca^{2+} permeability is not affected by the A149V mutation, and thus either conductance or open probability may explain the elevated Ca^{2+} conductance

The MEC-4(A149V) substitution may impact channel permeability to Ca^{2+}, open probability, or Ca^{2+} conductance. As a first step toward distinguishing among these possibilities, we determined the reversal potential of the current when oocytes were perfused with $CaCl_2$. The reversal potential is dictated by the permeability of the permeating ions bathing the extracellular and intracellular side of the membrane (Na^+ and Ca^{2+}) and by their concentrations. We found that the reversal potential of currents produced by the expression of MEC-4(d) + MEC-10(d) channel was not statistically different from the reversal potential of currents produced by the expression of MEC-4(A149V) + MEC-10(d) channel (Figure 6e), indicating that Ca^{2+} permeability of the MEC-4(A149V)- and MEC-4(d)-containing channel complexes is similar. Remaining mechanistic possibilities are that channel conductance and/or open probability of MEC-4(A149V) channels may be different depending on the permeating ion, alternatives that can be addressed in single channel experiments.

Overall, our electrophysiological studies indicate that combinatorial neurotoxicity is correlated with elevated Ca^{2+} and Na^{+} currents in the MEC-4(A149V) + MEC-10(d) channel, by a mechanism probably associated with increased channel conductance and/or open probability.

Discussion

Here, we report on a DEG/ENaC channel hyperactivated by a novel mechanism in which two distinct channel subunit variants, each of which only marginally impacts channel activity on its own, interact to alter channel properties to a toxic end. Our data hold implications for *in vivo* structure relationships within the channel class and convey insight into the mechanisms of neurotoxicity likely to apply across phyla.

The MEC-4(A149V) subunit is neurotoxic only in combination with MEC-10(d). Our genetic data establish that neither the homomeric MEC-4(A149V) channel nor the heteromeric MEC-4(A149V) + MEC-10(+) channel induces neurodegeneration *in vivo*, indicating that these channel configurations do not hyperactivate currents to neurotoxic levels. Remarkably, MEC-4(A149V) actually forms a functional touch-transducing complex *in vivo* as evidenced by the normal touch sensitivity of *mec-4(bz301)* mutants. We conclude that the basically functional MEC-4(A149V) subunit interacts with a borderline-deleterious MEC-10(d) subunit to induce significant neurotoxicity. This is the first case of synthetic neurotoxicity, dependent on two mutant subunits, reported for the DEG/ENaC channel class and a clear example in which interactions between subunits can dramatically alter channel activity. Given the demonstrated contributions of ASIC1a channels to infarct size in mouse ischemia models, and ENaC channels to human hypertension, our data raise the possibility that allelic interactions among DEG/ENaC subunits may differentially predispose individuals to neuronal loss in stroke or to blood pressure dysregulation, suggesting the potential importance of evaluating channel variants in patients affected by these conditions.

An extracellular AA substitution impacts channel pore and gating properties. Precise execution of ion channel conduction, critical to nervous system function and dysfunction, is intimately tied to channel structure, and our findings hold implications for structure/activity of the DEG/ENaC channel class in physiological context. MEC-4(A149) is an extracellular residue positioned 19 AAs away from the first transmembrane domain and adjacent to a conserved extracellular domain (MEC-4 AA 151–163; FPAITLCNLNPYK) (Figure 3a and b). Residues corresponding to MEC-4(A149) in other DEG/ENaC channel subunits are most commonly Ala or a hydrophobic residue (including Val, consistent with our finding that the MEC-4A149V mutant subunit is actually functional *in vivo;* see Figure 3b and Supplementary Figure 1). Little site-directed mutagenesis has probed the function of the adjacent FPAITLCNLNPYK region in the channel class, and no *mec-4*-disrupting mutations reported to date affect this region. Regions more C-terminal to the FPAITLCNLNPYK domain in mammalian DEG/ENaCs include a protease recognition site and a toxin-binding site (ASIC1a).[21–23] Studies on these domains, as well as genetic analysis of a more distant domain in *C. elegans* MEC-4 and DEG-1 that negatively regulates channel activity,[16] implicate multiple regions of the large extracellular domain of DEG/ENaCs in influencing channel properties.

How might extracellularly positioned MEC-4(A149) interact with the pore-associated MEC-10(d) subunit to alter channel conductance properties? The ASIC1a channel structure suggests that MEC-4(A149) and MEC-10(d) should not be in close proximity, at least in the desensitized state.[3] Thus, AA changes at these sites might induce conformational changes transmitted across the channel structure. Indeed, MEC-4(A149) corresponds to ASIC1a(T87), which contributes to a β-sheet structure that forms intrasubunit and intersubunit solvent-filled cavities,[3] and has been suggested to undergo extensive structural change during gating.[24]

Considering relative roles of Na^{+} and Ca^{2+} in neurotoxicity. In *Xenopus* oocytes, we found that the homomeric MEC-4(A149V) channel is permeable to Na^{+} but not to Ca^{2+}. Na^{+} conductance in this mutant channel is approximately 10-fold elevated compared with the native MEC-4(+) channel (Figure 6b and Goodman *et al.*[11]), although the overall current is still small ($\sim$1 μA). If there is a modest increase in Na^{+} current in the *in vivo* MEC-4(A149V) channel, it does not suffice to disrupt normal touch receptor function in the *mec-4(bz301)* mutant. Although we cannot rule out that channel properties *in vivo* might differ from those of the heterologously expressed channels, our observations suggest that (1) that MEC channels might not need to be permeable to Ca^{2+} ions to transduce touch sensation; and (2) larger currents through the MEC channels might not necessarily cause neurodegeneration if the channel is not permeable to Ca^{2+}. Our data also suggest that AAs corresponding to the MEC-4(A149) position in ASIC and ENaC channels may contribute to modulating channel conductance properties.

Genetic and physiological studies have previously suggested that Ca^{2+} permeability might be a critical factor in MEC-4(d) channel neurotoxicity.[13,15] Although the combination channel is hyperactivated for both Na^{+} and Ca^{2+} currents, Ca^{2+} conductance appears increased disproportionately to Na^{+} conductance in the heteromeric MEC-4(A149V) + MEC-10(d) channel, as compared with the MEC-4(d) + MEC-10(d) channel (Na^{+} and Ca^{2+} currents are 8 and 25%, respectively, of currents generated by the expression of *mec-4(d)* + *mec-10(d)*; Figure 6c and d). The relative change in ion conductance could result from an increase in Ca^{2+} conductance in the MEC-4(A149V) channel or an increase in Na^{+} conductance in the MEC-4(d) channels.

Although we cannot separate Na^{+} from Ca^{2+} conduction in these channels *in vivo*, our combined data suggest that Ca^{2+} permeability may be an essential factor in neurotoxicity. First, only the channels that exhibit significant Ca^{2+} currents in the oocyte expression system (MEC-4(d) and MEC-4 (A149V)-containing channels) induce neurodegeneration *in vivo*,[13] and this general observation extends to the neurotoxic ASIC1a channel.[2,14] Second, we note that the Na^{+}

currents conducted by the MEC-4(A149V) + MEC-10(d) mutant channel are as large as Na^+ currents produced by the MEC-4(A713V,G717E) mutant channel we previously characterized, which is not neurotoxic *in vivo*;[13] the Ca^{2+} currents of the MEC-4(A149V) + MEC-10(d) mutant channel, however, are larger than that of MEC-4(A713V,G717E). Thus, our data may have identified a threshold calcium conductance that correlates with *in vivo* neurotoxicity.

Finally, we have shown that necrosis progression induced by the combined *C. elegans* mutant subunits requires calreticulin function for neurotoxicity. This requirement supports a necrotic rather than apoptotic death mechanism[25] and suggests that the *in vivo* calcium conductance of the MEC-4(A149V) + MEC-10(d) channel is above the threshold for calcium-dependent catastrophic ER calcium release.

In summary, our data provide *in vivo* evidence in support of conformational changes exerted across the extracellular domain of DEG/ENaCs to impact multiple channel properties, contributing to the emerging picture of a dynamic and complex extracellular domain for the DEG/ENaC channel class. Our data also further support a role for elevated calcium conductance for the neurotoxic properties of dysregulated DEG/ENaC channels, and add mechanistic detail to an understanding of necrosis-initiating conditions, relevant to problems of neuronal loss in stroke and ischemia. Continued analysis of structure/activity in physiological context should expand the understanding of the potential for modulation of DEG/ENaC extracellular domains for potential therapeutic application.

Materials and Methods

Genetic strains and nematode growth. Nematode strains were maintained at 20°C on standard nematode growth medium (NGM) seeded with *Escherichia coli* strain OP50 as food source,[26] unless otherwise stated. *mec-4(d) = mec-4(u231)* encodes the neurotoxic MEC-4(A713V) substitution[8] and *mec-10(d)* encodes MEC-10(A673V).[9] Strains used were **WT** Bristol N2; ***mec-4(u231) X*** (*mec-4(d)*) (19); ***mec-10(tm1552) X*** (*mec-10*-null); ***crt-1(bz29)*** (calreticulin null);[15] **ZB154** *zdIs5[p_{mec-4}GFP] I* (25); **TU2562** *dpy-20(e1282) IV*; *uIs22[mec-3::gfp dpy-20(+)]* (42); **ZB2356** *bzIs67[p_{mec-10}mec-10(d)::GFP + pRF4(rol-6(su1006))] X*, abbreviated in following list as *bzIs67[mec-10(d)]*; **ZB2394** *zdIs5*; *bzIs67[mec-10(d)]*; **ZB2374** *bzIs75[p_{mec-4}mec-10(d)::GFP + unc-119(+)] IV*, abbreviated in following list as *bzIs75[mec-10(d)]*; **ZB2451** *zdIs5; uIs22 bzIs75[mec-10(d)]*; **ZB2513** *bzEx170[p_{mec-4}mec-4(bz301) + pRF4(rol-6(su1006))]*; *zdIs5; uIs22 bzIs75[mec-10(d)]*; **ZB2528** *bzEx177[p_{mec-4}mec-4(+) + pRF4(rol-6(su1006))]*; *zdIs5; uIs22 bzIs75[mec-10(d)]*. Double-mutant strains were constructed by standard genetic approaches.

mec-10(tm1552) was provided by the Japan National Bioresources Consortium (Dr. Shohei Mitani, unpublished observations) and has a ~0.45 kb deletion that removes sequences from exon 5 and part of exon 6, creating frameshift with a stop codon very close to the deletion site. No *mec-10* transcripts can be detected by reverse transcription-polymerase chain reaction (RT-PCR) in this background. We used primers with sequence 5′-GTAGGGTCTGCAACTAGCTC-3′ and 5′-TGGGAGGGAGCTTCATCTTA-3′ to identify the deleted genome. This strain was outcrossed 6 × before analysis and further genetic constructions.

Strain ZB2356 *bzIs67[p_{mec-10}mec-10(d)::GFP + pRF4(rol-6(su1006))] X* was constructed by co-injecting plasmid p_{mec-10}*mec-10(d)::GFP* and pRF4(*rol-6(su1006)*) into the WT N2 strain, selecting roller transformants and X-ray irradiating transgenics to identify stably transformed lines as described.[27] Integrated lines were outcrossed at least 6 × before further constructions or analysis. *bzIs67* appeared X-linked because crossing *bzIs67* males to N2 hermaphrodites yielded 50 : 50 males that were non-Rol. Single nucleotide polymorphism (SNIP) mapping[28] positioned *bzIs67* at approximately +10 on the X chromosome. The mutagenesis strain ZB2394 *zdIs5[p_{mec-4}GFP] I*; *bzIs67[p_{mec-10}mec-10(d)::GFP* + pRF4(*rol-6 (su1006))] X* was constructed using standard genetic approaches. The strain ZB2374 *bzIs75[p_{mec-4}mec-10(d)::GFP + unc-119(+)] IV* was created by the microparticle bombardment method as described.[29] Integrated lines were outcrossed at least four times before further constructions. SNIP mapping[28] positioned *bzIs75* on chromosome IV. For the verification of the molecular identity of *bz301*, we injected *pmec-4(bz301)* + pRF4(*rol-6(su1006)*) and *pmec-4(+)* + pRF4(*rol-6(su1006)*) into ZB2451 *zdIs5; uIs22 bzIs75[mec-10(d)]* strain to make ZB2513 *bzEx170[p_{mec-4}mec-4(bz301)* + pRF4(*rol-6(su1006))]*; *zdIs5*; *uIs22 bzIs75[mec-10(d)]* and ZB2528 *bzEx177[p_{mec-4}mec-4(+)* + pRF4(*rol-6(su1006))];zdIs5*; *uIs22 bzIs75[mec-10(d)]*.

Genetic screen for enhancers of *mec-10(d)*-induced cell death. We used nematode strain ZB2394, harboring the *mec-10(d)* transgene and expressing a GFP transgene (p_{mec-4}GFP) exclusively in touch neurons in our screen for necrosis enhancers. In this strain, almost all six touch neurons survive and fluoresce. We mutagenized L4/young adult animals using EMS according to standard protocols.[26] We distributed 30 F1 progeny to 15 cm × 15 cm plates and allowed animals to self-fertilize. Four days later, we screened F2 animals from each plate for the loss of touch cell fluorescence using a COPAS BIOSORT (Complex Object Parametric Analyzer and Sorter) from Union Biometrica (Holliston, MA, USA). We cloned out individuals with fewer than six fluorescent touch cells to create stocks of candidate homozygous suppressor mutants in which most of the population harbored <6 fluorescent touch cells (maximum of one line finally selected per mutagenesis plate to insure independent origin). We mapped *bz301* using standard procedures[26] (using *bzIs67* as X chromosome marker) and we identified the nucleotide change associated by DNA sequence of PCR products (GENEWIZ Inc., South Plainfield, NJ, USA).

General microscopy and touch assay. We scored for PLM GFP signals by observing the tails of L4 stage larvae with fluorescence dissection microscopy. We scored for swollen necrotic-like PLM touch neurons by examining tails of L1 stage larvae with DIC microscopy as previously described.[30] We took digital photographs through a Zeiss Axioplan 2 microscope after immobilizing L4 worms with 10 mM levamisol and placing on a 2% agarose pad. We performed gentle touch tests by stroking the body at anterior and posterior positions with an eyelash as described.[7]

Molecular biology. We constructed the p_{mec-10}*mec-10*::*GFP* plasmid by introducing a *PstI–BamHI* fragment, including the *mec-10* promoter and coding sequences except for those encoding the last three AAs, into pPD95.77 vector, which includes enhanced GFP (Fire Lab Vector Kit[31]). We then used the Quick Change Site Directed Mutagenesis Kit from Stratagene to change the AA at position 673 to generate p_{mec-10}*mec-10(d)*::*GFP* (oligos used: 5′-GTAAAAATGATGGT TGATTTTGGAGGACACCTTGGACTTTGGTC-3′ and 5′-GACCAAAGTCCAAGGT GTCCTCCAAAATCAACCATCATTTTTAC-3′). We constructed p_{mec-4}*mec-10(d)*::*GFP* by subcloning a 1.02 kb *StuI–ClaI* fragment containing the *mec-4* promoter into p_{mec-10}*mec-10(d)*::*GFP* to replace the *mec-10* promoter. *StuI–ClaI* restriction sites on the fragment were introduced by PCR using the following primers: 5′-GAAGGCCTAAGCTTCAATACAAGCTCAAATAC-3′ and 5′-CCATCGATTCCC TCTATAACTTGATAGCGATA-3′. p*mec-4* was described by Hong and Driscoll[32] and constructed by subcloning a 6.1 kb *HindIII–HindIII* fragment containing genomic *mec-4* promoter and coding sequences into pBluescript KS(−).[8] We constructed the p*mec-4(bz301)* by site-directed mutagenesis (Quick Change Site Directed Mutagenesis Kit from Stratagene) using the p*mec-4* plasmid as template (oligos used: 5′-CCAGACACTGTACCTTTTCCAGCAATTACGCTTTG-3′ and 5′-CAAAGC GTAATTGCTGGAAAAGGTACAGTGTCTGG-3′).

For channel assays in *Xenopus* oocytes, we used *mec-2*, *mec-6*, *mec-4(d)*, and *mec-10(d)* cDNAs subcloned into pGEM-HE or pSGEM, a gift from the Chalfie Lab described by Chelur *et al.*,[10] Goodman *et al.*,[11] and Bianchi *et al.*[13] We amplified cRNAs using the SMC4 bacterial strain.[11] We introduced the MEC-4(A149V) substitution into the PGEM + *mec-4* cDNA clone[11] by site-directed mutagenesis (Quick Change Site Directed Mutagenesis Kit, Stratagene), using oligos: 5′-GAA ATTTGACACTGTACCTTTTCCAGCAATTACGC-3′ and 5′-GCGTAATTGCTGGAA AAGGTACAGTGTCAAATTTC-3′.

Oocyte expression and electrophysiology. We synthesized capped RNAs using T7 mMESSAGE mMACHINE kit (Ambion), purified on Qiagen RNAeasy columns, and ran on denaturating agarose gels to check for size and cRNA integrity. We quantified cRNA by spectroscopy. We manually defolliculated stage V–VI oocytes after selecting them among multistaged oocytes dissected by

2 h collagenase treatment (2 mg/ml in Ca^{2+}-free OR2 solution) from *Xenopus laevis* ovaries (NASCO). We incubated oocytes in OR2 media, which consists of 82.5 mM NaCl, 2.5 mM KCl, 1 mM $CaCl_2$, 1 mM $MgCl_2$, 1 mM Na_2HPO_4, 0.5 g/l polyvinyl pyrolidone and 5 mM HEPES (pH 7.2), supplemented with penicillin and streptomycin (0.1 mg/ml) and 2 mM Na-pyruvate. The following day we injected oocytes with 52 nl of cRNA mix for a final amount of 5 ng per oocyte of each cRNA except for MEC-6, which we injected at the concentration of 1 ng per oocyte. We then incubated oocytes in OR2 at 20°C for 4 days before recording. We measured currents 4–10 days after cRNA injection using a two-electrode voltage clamp amplifier (GeneClamp 500B, Axon Instruments) at room temperature. Electrodes (0.3–1 M) were filled with 3 M KCl and we perfused oocytes with a NaCl solution containing (in mM): NaCl (100), KCl (2), $CaCl_2$ (1), $MgCl_2$ (2), HEPES (10), pH 7.2 or with a $CaCl_2$ solution containing $CaCl_2$ (73), KCl (2), HEPES (10), pH 7.2. We obtained chemicals from Sigma and Calbiochem. We used the pCLAMP suite of programs (Axon Instruments) for data acquisition and analysis. Currents were filtered at 200 Hz and sampled at 1 kHz.

Acknowledgements. We thank the Japan National Bioresource Project and Dr. Shoehi Mitani for the *mec-10* deletion, and Dr. Scott Clark for the *zdIs5* line. The *C. elegans* Genetic Stock Center provided some strains used for mapping. This work was supported by research grants from the NJ Commission on Spinal Cord Research to WZ (04-2902-SCR-E-0 and 06-2916-SCR-E-0); NIH Grant R01 NS034435 to MD and NIH Grant R21 NS049511 to LB.

1. Sattler R, Tymianski M. Molecular mechanisms of glutamate receptor-mediated excitotoxic neuronal cell death. *Mol Neurobiol* 2001; **24**: 107–129.
2. Xiong ZG, Zhu XM, Chu XP, Minami M, Hey J, Wei WL *et al.* Neuroprotection in ischemia: blocking calcium-permeable acid-sensing ion channels. *Cell* 2004; **118**: 687–698.
3. Jasti J, Furukawa H, Gonzales EB, Gouaux E. Structure of acid-sensing ion channel 1 at 1.9 A resolution and low pH. *Nature* 2007; **449**: 316–323.
4. Kellenberger S, Schild L. Epithelial sodium channel/degenerin family of ion channels: a variety of functions for a shared structure. *Physiol Rev* 2002; **82**: 735–767.
5. Suzuki H, Kerr R, Bianchi L, Frøkjaer-Jensen C, Slone D, Xue J *et al. In vivo* imaging of *C. elegans* mechanosensory neurons demonstrates a specific role for the MEC-4 channel in the process of gentle touch sensation. *Neuron* 2003; **39**: 1005–1017.
6. O'Hagan R, Chalfie M, Goodman MB. The MEC-4 DEG/ENaC channel of *Caenorhabditis elegans* touch receptor neurons transduces mechanical signals. *Nat Neurosci* 2005; **8**: 43–50.
7. Chalfie M, Sulston J. Developmental genetics of the mechanosensory neurons of *Caenorhabditis elegans*. *Dev Biol* 1981; **82**: 358–370.
8. Driscoll M, Chalfie M. The *mec-4* gene is a member of a family of *Caenorhabditis elegans* genes that can mutate to induce neuronal degeneration. *Nature* 1991; **349**: 588–593.
9. Huang M, Chalfie M. Gene interactions affecting mechanosensory transduction in *Caenorhabditis elegans*. *Nature* 1994; **367**: 467–470.
10. Chelur DS, Ernstrom GG, Goodman MB, Yao CA, Chen L, O'Hagan R *et al.* The mechanosensory protein MEC-6 is a subunit of the *C. elegans* touch-cell degenerin channel. *Nature* 2002; **420**: 669–673.
11. Goodman MB, Ernstrom GG, Chelur DS, O'Hagan R, Yao CA, Chalfie M. MEC-2 regulates *C. elegans* DEG/ENaC channels needed for mechanosensation. *Nature* 2002; **415**: 1039–1042.
12. Emtage L, Gu G, Hartwieg E, Chalfie M. Extracellular proteins organize the mechanosensory channel complex in *C. elegans* touch receptor neurons. *Neuron* 2004; **44**: 795–807.
13. Bianchi L, Gerstbrein B, Frøkjaer-Jensen C, Royal DC, Mukherjee G, Royal MA *et al.* The neurotoxic MEC-4(d) DEG/ENaC sodium channel conducts calcium: implications for necrosis initiation. *Nat Neurosci* 2004; **7**: 1337–1344.
14. Yermolaieva O, Leonard AS, Schnizler MK, Abboud FM, Welsh MJ. Extracellular acidosis increases neuronal cell calcium by activating acid-sensing ion channel 1a. *Proc Natl Acad Sci USA* 2004; **101**: 6752–6757.
15. Xu K, Tavernarakis N, Driscoll M. Necrotic cell death in *C. elegans* requires the function of calreticulin and regulators of Ca(2+) release from the endoplasmic reticulum. *Neuron* 2001; **31**: 957–971.
16. Garcia-Anoveros J, Ma C, Chalfie M. Regulation of *Caenorhabditis elegans* degenerin proteins by a putative extracellular domain. *Curr Biol* 1995; **5**: 441–448.
17. Hong K, Mano I, Driscoll M. *In vivo* structure–function analyses of *Caenorhabditis elegans* MEC-4, a candidate mechanosensory ion channel subunit. *J Neurosci* 2000; **20**: 2575–2588.
18. Royal DC, Bianchi L, Royal MA, Lizzio Jr M, Mukherjee G, Nunez YO *et al.* Temperature-sensitive mutant of the *Caenorhabditis elegans* neurotoxic MEC-4(d) DEG/ENaC channel identifies a site required for trafficking or surface maintenance. *J Biol Chem* 2005; **280**: 41976–41986.
19. Bianchi L, Driscoll M. The molecular basis of touch sensation as modeled in *Caenorhabditis elegans*. In: Stephan Frings, Jonathan Bradley (eds) *Transduction Channels in Sensory Cells*, Wiley: Weinheim, Germany, 2004, pp 1–30.
20. Brown AL, Fernandez-Illescas SM, Liao Z, Goodman MB. Gain-of-function mutations in the MEC-4 DEG/ENaC sensory mechanotransduction channel alter gating and drug blockade. *J Gen Physiol* 2007; **129**: 161–173.
21. Poirot O, Vukicevic M, Boesch A, Kellenberger S. Selective regulation of acid-sensing ion channel 1 by serine proteases. *J Biol Chem* 2004; **279**: 38448–38457.
22. Vukicevic M, Weder G, Boillat A, Boesch A, Kellenberger S. Trypsin cleaves acid-sensing ion channel 1a in a domain that is critical for channel gating. *J Biol Chem* 2006; **281**: 714–722.
23. Chen X, Kalbacher H, Grunder S. Interaction of acid-sensing ion channel (ASIC) 1 with the tarantula toxin psalmotoxin 1 is state dependent. *J Gen Physiol* 2006; **127**: 267–276.
24. Cushman KA, Marsh-Haffner J, Adelman JP, McCleskey EW. A conformation change in the extracellular domain that accompanies desensitization of acid-sensing ion channel (ASIC) 3. *J Gen Physiol* 2007; **129**: 345–350.
25. Chung S, Gumienny TL, Hengartner MO, Driscoll M. A common set of engulfment genes mediates removal of both apoptotic and necrotic cell corpses in *C. elegans*. *Nat Cell Biol* 2000; **2**: 931–937.
26. Brenner S. The genetics of *Caenorhabditis elegans*. *Genetics* 1974; **77**: 71–94.
27. Rosenbluth RE, Cuddeford C, Baillie DL. Mutagenesis in *Caenorhabditis elegans* II. A spectrum of mutational events induced with 1500 r of gamma-radiation. *Genetics* 1985; **109**: 493–511.
28. Wicks SR, Yeh RT, Gish WR, Waterston RH, Plasterk RH. Rapid gene mapping in *Caenorhabditis elegans* using a high density polymorphism map. *Nat Genet* 2001; **28**: 160–164.
29. Praitis V, Casey E, Collar D, Austin J. Creation of low-copy integrated transgenic lines in *Caenorhabditis elegans*. *Genetics* 2001; **157**: 1217–1226.
30. Driscoll M. Methods for the study of cell death in the nematode *Caenorhabditis elegans*. *Methods Cell Biol* 1995; **46**: 323–353.
31. Mello C, Fire A. DNA transformation. *Methods Cell Biol* 1995; **48**: 451–482.
32. Hong K, Driscoll M. A transmembrane domain of the putative channel subunit MEC-4 influences mechanotransduction and neurodegeneration in *C.elegans*. *Nature* 1994; **367**: 470–473.

Supplementary Information accompanies the paper on Cell Death and Differentiation website (http://www.nature.com/cdd)